Comprehensive Topological Analyses of Isolated Resonant Converters in PEV Battery Charging Applications

Haoyu Wang, *Student Member, IEEE*, and Alireza Khaligh, *Senior Member, IEEE*

Power Electronics, Energy Harvesting and Renewable Energies Laboratory
Electrical and Computer Engineering Department and Institute for Systems Research
University of Maryland; College Park, MD 20742
Email: khaligh@ece.umd.edu; URL: www.ece.umd.edu/~khaligh

***Abstract*—In this paper, four basic resonant dc/dc topologies (SRC, PRC, LCC, and LLC) are investigated for plug-in electric vehicle (PEV) charging applications. A methodology based on first harmonic approximation is introduced to effectively evaluate the circuit performance in battery charging applications. The charging profile of a 360 V, 3.2 kW Li-ion battery pack is introduced to facilitate the design of resonant chargers. Four half-bridge isolated resonant chargers are designed and compared using this proposed method. Simulations show that LLC resonant converter outperforms the other three converters by maintaining good performance over the full range of battery states of charge.**

***Index Terms*—battery chargers, dc/dc conversion, on-board chargers, plug-in electric vehicle, resonant converters.**

I. Introduction

In on-board plug-in electric vehicle (PEV) battery chargers, an ultra-compact, highly efficient isolated dc/dc converter is desired for battery current regulation and galvanic isolation.

In comparison to conventional pulse width modulation (PWM) converters, frequency modulated resonant converters exhibit advantages such as (a) reduced switching losses and thus higher conversion efficiency, (b) capability to operate at higher switching frequency, which helps to reduce the size of magnetic components and thus to improve the power density, and (c) zero-voltage switching feature, which can eliminate some sources of electromagnetic interference [1], [2]. Consequently, resonant dc/dc converters are deemed as a good candidate for front-end dc/dc conversion applications, which requires a constant output voltage [3–5].

In PEV battery charging applications, the battery voltage and load condition vary in a wide range depending on the different state of charge (SOC) of the battery, as well as different battery types [6], [7]. Therefore, operating with maximum efficiency through reducing the conduction and switching losses over the full output voltage and load ranges is a challenging issue in isolated resonant charger design.

Based on the differences in the resonant tank and its relationship with the load, resonant dc/dc topologies are classified into four categories, (a) series resonant converter (SRC), (b) parallel resonant converter (PRC), (c) LCC series-parallel resonant converter (LCC), and (d) LLC series-parallel resonant converter (LLC). Fig. 1 illustrates these four types of isolated half-bridge resonant topologies, which may be used for on-board PEV charging applications.

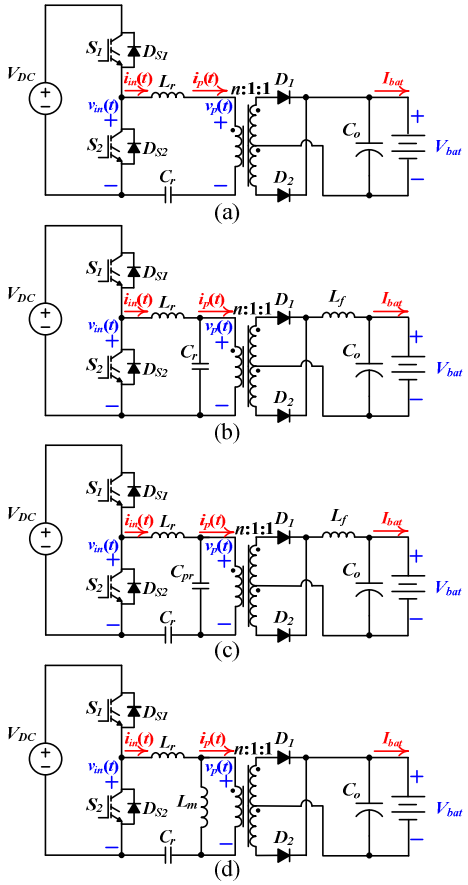

Fig.1. Isolated resonant topologies in battery charging applications. (a) Series resonant converter (SRC). (b) Parallel resonant converter (PRC). (c) LCC series-parallel resonant converter (LCC). (d) LLC series-parallel resonant converter (LLC).

In this paper, these four isolated half-bridge resonant converters (SRC, PRC, LCC, and LLC) are investigated and evaluated for PEV battery charging applications. It is shown that that LLC could maintain good efficiency performance over a wide range of battery SOCs.

This paper is organized as follows; Section II details the analysis methodology of resonant converters. Section III explains the charging profiles of a Li-ion battery pack. Section IV illustrates the basic design and comparison considerations of

978-1-4799-0148-7/13/$31.00 ©2013 IEEE

resonant converters. In Section V, the resonant converters in PEV battery charging applications are compared. Finally, Section VI summarizes the study and features the benefits based on the achieved results.

II. Circuit Modeling and Converter Analyses

As demonstrated in Fig. 1, each topology consists of four parts: (a) a dc voltage source and switch network, which operate as a square wave generator, (b) a resonant tank, (c) a center-tapped transformer and half-bridge rectifier, and (d) a low-pass filter network and dc load, which is a battery pack.

A. Circuit modeling

According to Fourier Series, the square wave, $v_{in}(t)$, contains dc component, first harmonic, and higher odd harmonics as shown in Eq. (1),

$$v_{in}(t)=\frac{V_{DC}}{2}+\frac{2V_{DC}}{\pi}\sin(2\pi f_s t)+\sum_{n=3,5,7,\ldots}\frac{2V_{DC}}{n\pi}\sin(2\pi n f_s t) \quad (1)$$

where, f_s is the switching frequency and also the frequency of first harmonic component. $v_{in}(t)$ is fed to the input terminals of the resonant tank. The primary resonant frequency of the resonant tank, f_p, is the resonant frequency between L_r and C_r,

$$f_p=\frac{1}{2\pi\sqrt{L_r C_r}} \quad (2)$$

In order to optimize the conversion efficiency, f_p is tuned to be close to desired switching frequency. Thus, the resonant tank works like a filter, which filters the higher odd harmonics of $v_{in}(t)$. To simplify the analysis, only the response of first harmonic is considered in the circuit analysis. This approach is named first harmonic approximation.

Using first harmonic approximation, the network consists of center-tapped transformer, half-bridge rectifier, low-pass filter, and dc load (battery) could be modeled as an ac resistor. By calculating the root mean square values of its input voltage and current, the equivalent ac resistance, R_{ac}, could be found as,

$$R_{ac}=\frac{8n^2}{\pi^2}\times R_L=\frac{8n^2}{\pi^2}\frac{V_{bat}}{I_{bat}} \quad (3)$$

Where, n is the turns ratio of the center-tapped transformer, V_{bat} and I_{bat} are the battery voltage and charging current, respectively. Detailed derivations could be found in [8].

By using the first harmonic approximation, and the equivalent load resistance R_{ac}, the circuit models of resonant converters are plotted in Fig. 2, where $v_{in,1}(t)$, $i_{in,1}(t)$, $v_{p,1}(t)$, and $i_{p,1}(t)$ denote the first harmonic components of input voltage $v_{in}(t)$, input current $i_{in}(t)$, voltage of the primary side of transformer $v_p(t)$ and the current of primary side of transformer $i_p(t)$, respectively.

B. Dc voltage and current characteristics

According to the ac equivalent models shown in Fig. 2, the normalized voltage gain, transconductance, and the conductance of the circuit could be derived as,

$$G_n=\frac{v_{p,1,rms}}{v_{in,1,rms}}=\left|\frac{Z_l}{Z_{in}}\right| \quad (4)$$

$$g_n=\frac{i_{p,1,rms}}{v_{in,1,rms}}=\left|\frac{Z_l}{Z_{in}}\right|\frac{1}{R_{ac}} \quad (5)$$

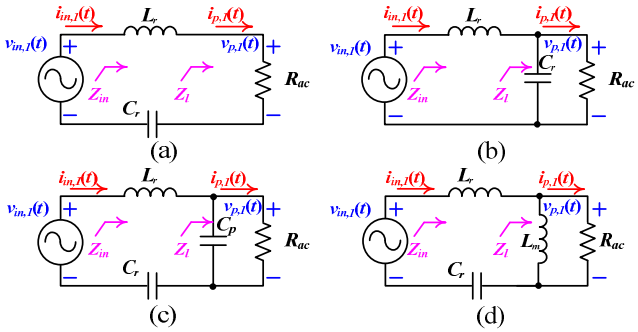

Fig. 2. Ac equivalent models of resonant converters. (a) SRC. (b) PRC. (c) LCC. (d) LLC.

$$C_n=\frac{i_{in,1,rms}}{v_{in,1,rms}}=\left|\frac{1}{Z_{in}}\right| \quad (6)$$

where, Z_l and Z_{in} are the input and load impedance of the ac equivalent model.

Accepting the accuracy of first harmonic approximation, the battery voltage, charging current and rms value of input current could be written as,

$$V_{bat}\approx\frac{v_{p,1,rms}}{v_{in,1,rms}}\frac{V_{DC}}{2n}=\left|\frac{Z_l}{Z_{in}}\right|\frac{V_{DC}}{2n} \quad (7)$$

$$I_{bat}=\frac{V_{bat}}{R_L}\approx\left|\frac{Z_l}{Z_{in}}\right|\frac{4n}{R_{ac}\pi^2} \quad (8)$$

$$i_{in,rms}\approx i_{in,1,rms}=\left|\frac{v_{in,1,rms}}{Z_{in}}\right|=\left|\frac{\sqrt{2}V_{DC}}{\pi}\right|\left|\frac{1}{Z_{in}}\right| \quad (9)$$

The dc voltage and current characteristics are critical figure of merits in analyzing the circuit performance in battery charging applications.

C. Capacitive and inductive operations

The input impedance of the resonant circuit, Z_{in}, could be capacitive or inductive. Due to the filtering effect of the resonant tank, the input current, $i_{in}(t)$, is approximated as a sinusoidal function. The waveforms of input voltage $v_{in}(t)$, and its first harmonic component $v_{in1}(t)$, as well as $i_{in}(t)$ are plotted in Fig. 3.

Fig. 3(a) shows the circuit operation in capacitive region. Z_{in} is capacitive, $i_{in}(t)$ leads $v_{in}(t)$ with certain phase difference ϕ_1. As seen in the figure, the turn-off process of switches (S_1&S_2) is soft switching. However, the turn-on process of switches, and the turn-off process of freewheeling diodes (D_{S1}&D_{S2}) are both hard switching. The reverse recovery process of freewheeling diodes leads to significant switching losses. Consequently, the freewheeling diodes must have good reverse-recovery characteristics to avoid large reverse spikes flowing through the switches, and to minimize the diode turn-off losses. In capacitive operation, MOSFETs in high switching frequency applications are not suitable as the primary switches. It is possible to use thyrisors in low switching frequency applications [9].

Fig. 3(b) illustrates the circuit operation in inductive region. Z_{in} is inductive, $i_{in}(t)$ lags $v_{in}(t)$ with certain phase difference ϕ_2. As seen in the figure, the turn-on process of switches, and the turn-off process of freewheeling diodes are both soft switching. However, the turn-off process of switches is hard switching. The reverse recovery losses from the freewheeling diodes are

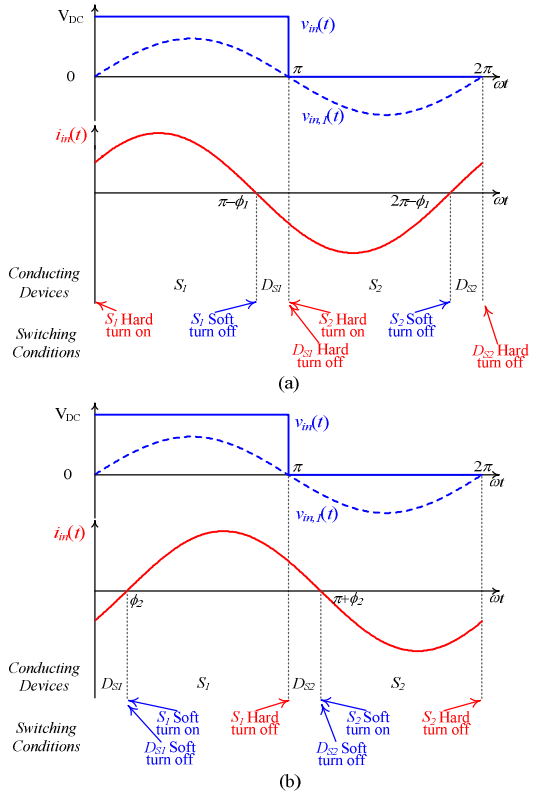

Fig. 3. Switching output waveforms in continuous conduction mode for resonant converters with (a) capacitive Z_{in}, and (b) inductive Z_{in}.

eliminated. The freewheeling diodes do not need to have very fast reverse-recovery characteristics. Thus, MOSFETs are suitable as primary switches in high switching frequency applications. Moreover, by paralleling small snubber capacitors directly with the switches, the turn-off losses of the switches could be eliminated.

Operating the converter in high switching frequency would reduce the size of energy storage components and effectively improve the energy density of the converter. Therefore, only MOSFETs in high frequency application and inductive operations are considered in the following analyses.

SRC and PRC are single resonance converters. f_p is the only resonance frequency of the resonant circuit. LCC has two resonance frequencies. f_p is the frequency of the primary resonance. $f_{s,LCC}$ is the frequency of the secondary resonance between L_r, C_r, and C_p. $f_{s,LCC}$ could be calculated as,

$$f_{s,LCC} = \frac{1}{2\pi\sqrt{L_r C_r C_p / \left(C_r + C_p\right)}} \tag{10}$$

Similar to LCC, LLC also has two resonance frequencies. f_p is the frequency of the primary resonance. $f_{s,LLC}$ is the frequency of the secondary resonance between L_r, L_m, and C_r. $f_{s,LCC}$ could be calculated as,

$$f_{s,LLC} = \frac{1}{2\pi\sqrt{C_r\left(L_r + L_m\right)}} \tag{11}$$

To illustrate different load conditions, quality factor Q is introduced. Q is defined to be the ratio between characteristic impedance ($\sqrt{L_r/C_r}$) and R_{ac}.

$$Q = \frac{\sqrt{L_r C_r}}{R_{ac}} \tag{12}$$

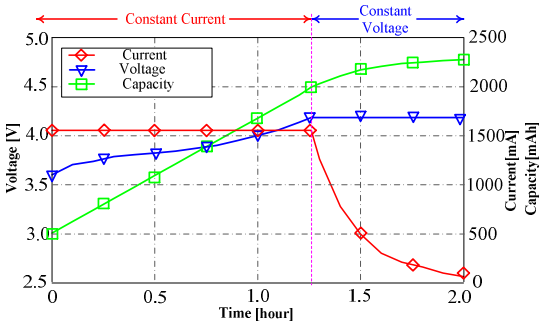

Fig.4. Charging characteristics of a Li-Ion battery cell.

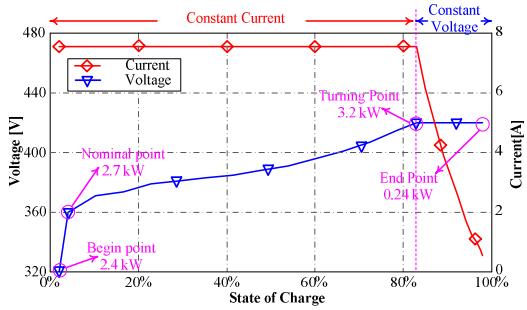

Fig. 5. Charging profile of a 360 V Li-Ion battery pack rated at 3.2 kW.

Large Q corresponds to small load resistance and heavy load condition. On the contrary, small Q corresponds to large load resistance and light load condition.

III. Charging Profile of Li-Ion Battery

A battery cell is an electrochemical unit, which stores chemical energy and converts it to electrical energy. Among suitable batteries for PEVs [10], Li-ion batteries have the advantage of higher energy densities, no memory effect, and only a slow loss of charge when not in use [11].Thus, Li-ion batteries are growing in popularity for PEV applications. In this paper, Li-ion battery is used as a case study to investigate the performance of resonance charger topologies.

Constant current (CC) and constant voltage (CC) charging is a commonly used charging strategy, which achieves fast charging while avoiding battery performance degradation [12]. Fig. 4 provides the charging characteristic of a single Li-ion battery cell. The battery cell has 3.6 V nominal voltage, and 2350 mAh capacity. A depleted battery is firstly charged with CC mode, and the voltage begins to increase. When the voltage reaches 4.2 V, the charging enters into CV mode, and the current begins to decrease. In the intersection between the CC mode and CV mode, the maximum charging power is achieved.

Based on the charging data of single battery cell, the charging profile of a Li-ion battery pack could be obtained, as plotted in Fig. 5. The charging power of this battery pack is rated at 3.2 kW. In the charging process, battery on the load side could be equivalent to a resistor, whose resistance is equal to battery voltage over charging current.

According to Fig. 5, there are four key points in the charging process. Begin point and end point correspond to the beginning and end of the charging process, respectively. At nominal point, the battery voltage is equal to the nominal voltage of the battery pack. Turning point marks the transition from CC to CV charging mode. Parameters of those four key points are summarized in Table I. The quality factors could be easily

TABLE I
KEY POINTS IN THE CHARGING PROFILE OF THE PEV BATTERY PACK

Parameter	Begin Point	Nominal point	Turning point	End point
V_{bat}	320V	360V	420V	420V
I_{bat}	7.56A	7.56A	7.56A	0.56A
P	2.4kW	2.7kW	3.2kW	0.24kW
R_L	42.3 Ω	47.6 Ω	55.6 Ω	750 Ω

calculated based on Eqs. (3) and (12).

In the following sections, the analyses of resonant converter topologies are based on the charging profile of this 360 V Li-ion battery pack.

IV. BASIC DESIGN AND COMPARISON CONSIDERATIONS

For the convenience of comparison, the dc link voltages and primary resonance frequencies are designed to be 600 V, and 200 kHz, respectively. MOSFTs are chosen as the primary switches. Thus, all the converters are designed to operate in inductive region.

According to previous analysis, in inductive operation, the turn-on of MOSFETs and the turn-off of freewheeling diodes are lossless. Besides, negligible losses are associated with the turn-on process of power diodes [1]. Hence, the dominant losses in inductive operation are conduction losses. Conduction losses are determined by the circulating energy in the resonant tank. High circulating energy in the resonant tank corresponds to high conduction loss. The circuit circulating power in the resonant tank could be calculated as,

$$P_c = \sum_{L=Lr,Lp} i_{L,rms}^2 j\omega L + \sum_{C=Cr,Cp} i_{C,rms}^2 \frac{1}{j\omega C} \quad (13)$$

By comparing the circulating power in the circuit, we are able to compare the related conduction losses in the converters.

At f_p, L_r and C_r resonate, and resonance impedance is zero. Thus, the circulating energy and consequently the conduction losses in L_r and C_r are minimized. However, with the increase of switching frequency (higher than f_p), the impedance of the resonant tank would increase. Thus, more energy would be circulated in the resonant tank instead of being transferred to the output [4]. The increased circulating energy increases the conduction losses and deteriorates the conversion efficiency. Usually, operating the converter in inductive region and closer to f_p would have smaller conduction losses and thus higher conversion efficiency.

Since the turn-off of MOSFETs is hard switching, the related switching losses are the second important source of converter losses. The switching losses in the semiconductor devices are proportional to the switching frequency. High switching frequency corresponds to high turning-off losses from the MOSFETs.

In this specific battery charging applications, the switching frequency at "nominal point" is designed to be close to f_p. Thus, operating close to "nominal point" incurs both small conduction losses and small switching losses. The worst conversion efficiency corresponds to the "end point", which has lightest load condition and highest switching frequency. Therefore, in designing resonant converter, the target is to optimize the circuit performance at the "end point", where the highest conduction losses and switching losses are expected.

Another important performance parameter of resonant converter is its short circuit protection capability. When short circuit happens, the power management module would boost the switching frequency to a higher value. Thus, the input impedance of the resonant tank would increase, which would limit the short circuit current.

TABLE II
PARAMETERS OF DESIGNED RESONANT CHARGERS

Parameter	SRC	PRC	LCC	LLC
n:1	2/3	2	1.1	1
C_r	10nF	15nF	15nF	15nF
L_r	63.3μH	42.2μH	42.2μH	42.2μH
C_p	n/a	n/a	14nF	n/a
L_m	n/a	n/a	n/a	42.2μH
Q range	0.29~ 5.22	0.022~ 0.39	0.072~ 1.28	0.087~ 1.55

Based on the aforementioned considerations, the aforementioned half bridge isolated resonant converters are designed and compared. Parameters of these circuits are provided in Table II. Comparisons are made in Section V.

V. COMPARISON OF RESONANT CONVERTERS IN PEV BATTERY CHARGING APPLICATIONS

A. Series resonant charger

Based on equations (4)-(9), the dc voltage and current characteristics of the SRC PEV battery charger are plotted in Fig. 6. Five curves correspond to five load conditions, which include those four key points in the charging process, as well as the short circuit condition. As seen in the figure, at f_p, SRC has the maximum voltage gain and operates as a constant voltage source. This is because the impedance of L_r and C_r is zero at f_p. The load voltage is equal to the input voltage. In order to provide some gain margin, this voltage is designed to be slightly higher than 420 V. With switching frequency higher than f_p, the impedance of the L_r dominates the impedance of the resonant tank, which makes the circuit inductive.

In CC charging mode, the switching frequency shifts from 219.9 kHz to 212.2 kHz. This means low circulating energy in the resonant tank and small conduction losses. Generally, SRC charger has good performance in the CC charging mode.

The second advantage of SRC battery charger is its good short circuit protection performance. As seen in Fig. 6, since the curve current at Q_{SC} is steep, it is easy to boost the switching frequency to control the short circuit current.

Since the load is series with the resonant tank, the current flowing through the load is equal to the current circulating in the resonant tank. This makes the circuiting power in the resonant tank small in CV mode. Thus, the conduction losses are also small. Let's takes the "end point" as an example. At "end point", switching frequency goes to 370 kHz while input rms current is 0.93 A. Since the impedance of L_r dominates the impedance of the resonant tank, circulating power could be approximated as,

$$P_c \approx i_{in,rms}^2 j\omega L_r = 84.9VA \quad (14)$$

This value is small in comparison to other topologies.

However, the critical defect of SRC lies in its unacceptable poor voltage regulation performance in light load condition. In light load condition, the slope of voltage curve is extremely small, which makes it hard to regulate the voltage.

Moreover, since the switching frequency is moved to a large value, this makes SRC suffer from high switching losses in CV charging mode. As a result, SRC is not a good candidate for

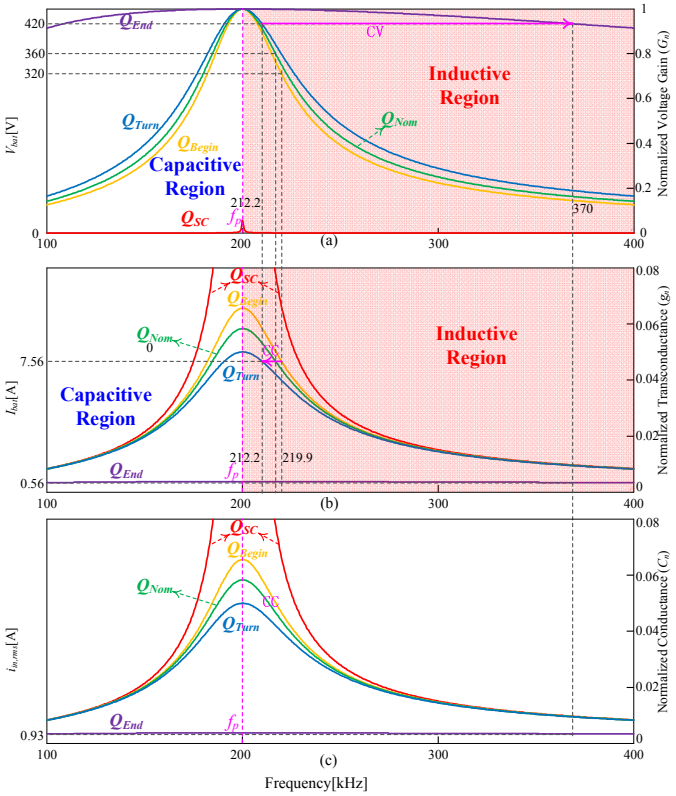

Fig. 6. Dc voltage and current characteristics of the SRC charger.

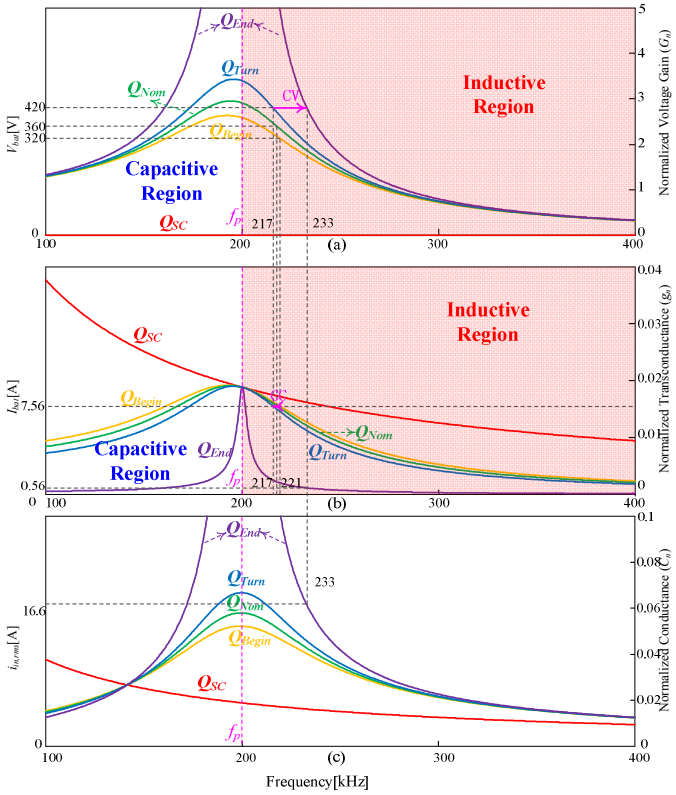

Fig. 7. Dc voltage and current characteristics of the PRC charger.

PEV battery charger.

B. *Parallel resonant charger*

Similarly, the dc voltage and current characteristics of the PRC PEV battery charger are plotted in Fig. 7. As seen in the figure, at f_p, PRC has the highest voltage gain in inductive region. The charging current is constant at f_p. In order to provide some margin, this current is designed to be slightly higher than 7.56 A. With switching frequency higher than f_p, the impedance of the L_r dominates the impedance of the resonant tank, which makes the circuit inductive.

In CC charging mode, the operating frequency shifts from 221 kHz to 217 kHz. This means low circulating energy in the resonant tank and small conduction losses. Similar to SRC, PRC charger also has good performance in the CC charging mode.

PRC battery charger also has good short circuit protection performance. When the short circuit happens, the input current would be limited by the impedance of L_r. As seen in Fig. 7, in inductive region, the short circuit current is always smaller than the constant current at f_p.

In constant voltage charging, the operating frequency shifts from 217 kHz to 233 kHz. As could be observed in Fig. 7, the input current is relatively independent on the load condition. This is the main disadvantage of PRC. This characteristic incurs its poor performance in light load or small quality factor condition. Let's take the "end point" as a simple example. At "end point", switching frequency is shifted to 233 kHz while input rms current is 16.6A. Since impedance of L_r dominates impedance of the resonant tank, circulating power could be approximated as,

$$P_c \approx i_{in,rms}^2 j\omega L_r = 17.0kVA \tag{15}$$

This value is much larger than that of SRC. Thus, most of the current is circulating in the resonant tank and does not contribute to the power delivered to the load. This means high conduction losses and low conversion efficiency. Consequently, PRC is not a good candidate for PEV battery charger.

C. *LCC series-parallel charger*

The dc voltage and current characteristics of the LCC PEV battery charger are plotted in Fig. 8. As seen in the figure, in the boundary between inductive and capacitive regions, LCC converter has the peak voltage gain. At f_p, LCC converter operates as a constant voltage source. While at $f_{s,LCC}$, LCC converter operates as a constant current source. In inductive region and within the same load line, both the voltage gain and transconductance decrease with the increase of switching frequency.

LCC is capacitive if the converter is operating below f_p, and is inductive if the converter is operating above $f_{s,LCC}$. In between f_p and $f_{s,LCC}$, capacitive or inductive nature of input impedance is determined by the load condition. In inductive region, the impedance of the L_r dominates the impedance of the resonant tank.

In CC charging mode, switching frequency shifts from 277 kHz to 276.9 kHz. This means the voltage is very sensitive to the load variation in CC charging mode. In comparison to PRC circuit, this frequency is further away from f_p. This means LCC converter has relatively high circulating energy in the resonant tank and large conduction losses in CC charging mode.

LCC battery charger also has good short circuit performance. When the short circuit happens, the input current is limited by the impedance of the inductance. As seen in Fig. 8(b), it is easy to limit the short circuit current by slightly boosting the switching frequency.

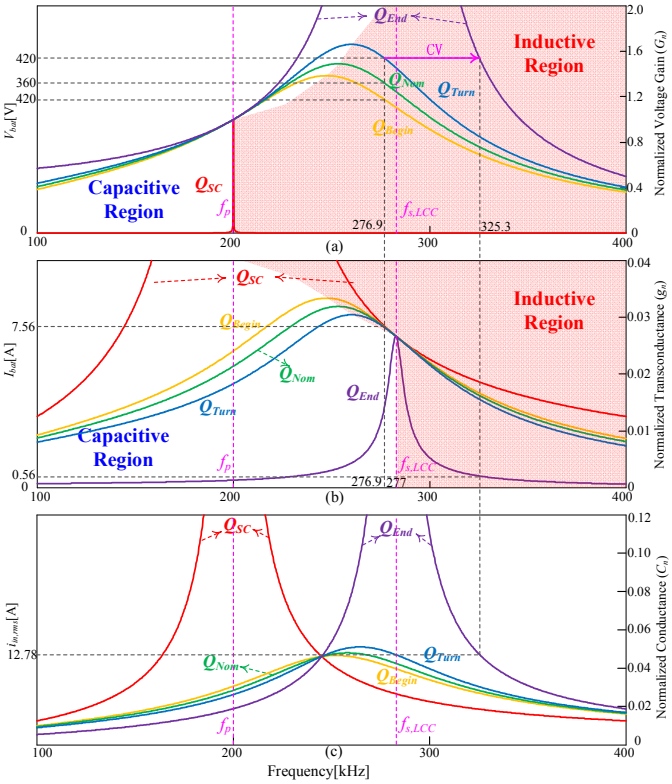

Fig. 8. Dc voltage and current characteristics of the LCC charger.

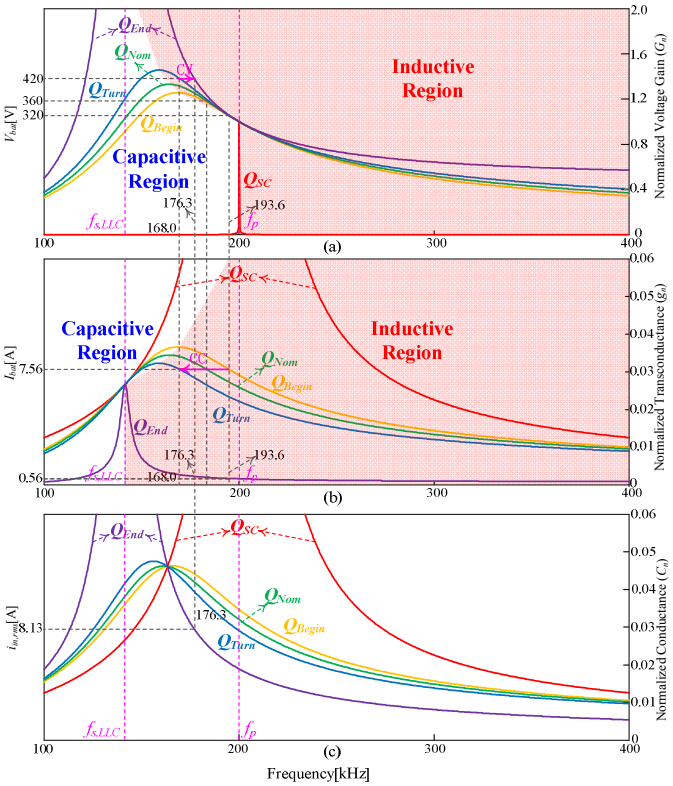

Fig. 9. Dc voltage and current characteristics of the LLC charger.

In CV charging mode, the operating frequency shifts from 276.9 kHz to 325.3 kHz. Similar to PRC, LLC also suffers from its poor performance in light load condition. This could be observed in Fig. 8. Let's take the "end point" as a simple example. At "end point", switching frequency goes to 325.3 kHz while input rms current is 12.78A. Since the impedance of L_r dominates the impedance of the resonant tank, the circulating power could be approximated as,

$$P_c \approx i_{in,rms}^2 j\omega L_r = 14.1kVA \tag{16}$$

This value is much larger than that of SRC and around the same level as that of PRC. Most of the current is circulating in the resonant tank and does not contribute to the power delivered to the load. This means high conduction losses and low conversion efficiency.

Actually, beyond the secondary resonance frequency ($f_{s,LCC}$), the LCC circuit behaves like a PRC converter. This is because at this condition, the impedance of L_r is much larger than the impedance of C_r, which makes L_r and C_r behave like an inductor. This explains why LCC circuit has the same problem as PRC circuit in light load condition. Hence, LCC is not a good candidate for PEV battery charger.

D. LLC series-parallel charger

The dc voltage and current characteristics of the LLC PEV battery charger are plotted in Fig. 9. As seen from the figure, in the boundary between inductive and capacitive regions, LLC converter has the peak charging current. At f_p, LLC converter operates as a constant voltage source. While at $f_{s,LLC}$, LLC converter operates as a constant current source. In inductive region and within the same load line, both the voltage gain and transconductance decrease with the increase of switching frequency.

LLC is capacitive if the converter is operating below $f_{s,LLC}$, and is inductive if the converter is operating above f_p. In between $f_{s,LLC}$ and f_p, capacitive or inductive are determined by the load condition. In inductive region, the impedances of the L_r and L_m dominate the impedance of the resonant tank.

In CC charging mode, the switching frequency shifts from 193.3 kHz to 168 kHz. In comparison to LCC circuit, this frequency is smaller and closer to f_p. This means LLC has relatively smaller circulating energy in the resonant tank and smaller conduction losses in CC charging mode than LCC. In CV charging, the operating frequency shifts from 276.9 kHz to 325.3 kHz. At light load condition, the slope of voltage curve is still big, which makes it easy to regulate the output voltage. This makes LLC outperform SRC.

The short circuit performance of LLC is not as good as the other three resonant converters, but it is sufficient to control the short circuit current. This is because beyond f_p, the impedance of inductors is large enough to regulate the short circuit current. As seen in Fig. 9(b), by boosting the switching frequency, the short circuit current could be successfully reduced to normal level.

The performance in light load condition of LLC is much better than PRC and LCC. This could be observed in Fig. 9. Let's take the "end point" as a simple example. At "end point", switching frequency goes to 176.3 kHz while input current is 8.13A. The circulating power could be calculated as,

$$P_c = i_{in,rms}^2 j\omega L_r + i_{in,rms}^2 \frac{1}{j\omega C_r} + i_{Lm,rms}^2 j\omega L_m = 1.79kVA \tag{17}$$

This value is much smaller than that of PRC and LCC. This means much less conduction losses and higher conversion efficiency in CV charging mode.

Moreover, the switching frequency of LLC is much smaller

TABLE III
COMPARISON OF RESONANT CONVERTERS IN PEV CHARGING APPLICATIONS

Performance	SRC	PRC	LCC	LLC
Voltage regulation capability at high SOC	Bad	Good	Good	Good
Additional filter inductor on secondary side	No	Yes	Yes	No
Frequency range in CC charging mode	219.9~212.2 kHz	221~217 kHz	277~276.9 kHz	193.6~167.3 kHz
Efficiency in CC charging mode	High	High	Moderate	High
Short circuit protection performance	Very good	Very good	Very good	Good
Frequency range in CV charging mode	212-370 kHz	217-233 kHz	276.9-325.3 kHz	168.0-176.3 kHz
Circulating energy at highest SOC	84.9 VA	17.0 kVA	14.1 kVA	1.79 kVA
Conduction losses in CV charging mode	Very small	Very large	Very large	Small
Conduction losses in CV charging mode	Large	Small	Moderate	Small
Efficiency in CV charging mode	Moderate	Low	Low	Moderate

than the other three topologies in the full load range. This means the LLC has the smallest switching losses among those four resonant converters.

The performances of SRC, PRC, LCC, and LLC chargers are summarized in Table III. It is clear that LLC has good performance in the full range of battery SOC. Thus, LLC is a more suitable candidate for PEV battery chargers.

VI. CONCLUSION

In this paper, four resonant topologies (SRC, PRC, LCC, and LLC) are analyzed and compared in terms of their performance characteristics for PEV battery charging applications. A new methodology is proposed to effectively evaluate the circuit performance in battery charging applications. This methodology includes evaluating the battery voltage, charging current, as well as the input rms current characteristics to design the resonant chargers and to compare the chargers' performance.

Using the proposed method, four half-bridge isolated resonant chargers, which are rated at 3.2 kW and used to charge a 360 V Li-ion battery pack, are designed and evaluated. Based on the analytical results, it is shown that LLC charger takes the advantages of LCC and PRC chargers, while avoiding the drawbacks of SRC chargers. LLC could maintain better efficiency, voltage regulation, as well as short circuit protection performance over the full range of battery SOC. Thus, LLC could be chosen as an excellent candidate for PEV battery charging applications.

ACKNOWLEDGEMENT

This work is supported in part by the Maryland Industrial Partnerships Program and CoolCAD Electronics LLC., which is gratefully acknowledged.

REFERENCES

[1] D. Erickson, R.W. and Maksimovic, *Fundamentals of power electronics*. Springer, 2001.

[2] R. L. Steigerwald, "A comparison of half-bridge resonant converter topologies," *IEEE Transactions on Power Electronics*, vol. 3, no. 2, pp. 174–182, Apr. 1988.

[3] F. C. Lee and A. J. Zhang, "LLC resonant converter for front end DC/DC conversion," in *Proc. IEEE Applied Power Electronics Conference and Exposition,* 2002, pp. 1108–1112.

[4] B. Yang, "Topology investigation for front end DC/DC power conversion for distributed power system," Virginia Polytechnic Institute and State University, 2003.

[5] F. Canales, P. Barbosa, and F. C. Lee, "A wide input voltage and load output variations fixed-frequency ZVS DC/DC LLC resonant converter for high-power applications," in *Proc. IEEE Industry Applications Conference,* 2002, pp. 2306–2313.

[6] C.-H. Lin, C.-M. Wang, M.-H. Hung, and M.-H. Li, "Series-resonant battery charger with synchronous rectifiers for $LiFePO_4$ battery pack," in *Proc. IEEE Conference on Industrial Electronics and Applications*, 2011, pp. 316–321.

[7] F. Musavi, M. Craciun, M. Edington, W. Eberle, and W. G. Dunford, "Practical design considerations for a LLC multi-resonant DC-DC converter in battery charging applications," in *Proc. IEEE Applied Power Electronics Conference and Exposition*, 2012, pp. 2596–2602.

[8] H. Huang, "Designing an LLC resonant half-bridge power converter," in *Texas Instruments 2010–2011 Power Supply Design Seminar*, 2011.

[9] T. M. Mohan, N. and Undeland, *Power electronics: converters, applications, and design*. Wiley, 2002.

[10] S. Dusmez, A. Cook, and A. Khaligh, "Comprehensive analysis of high quality power converters for level 3 off-board chargers," in *Proc. 2011 IEEE Vehicle Power and Propulsion Conference*, 2011.

[11] "ThermoAnalytics□: HEV Vehicle Battery Types." [Online]. Available: http://www.thermoanalytics.com/support/publications/batterytypesdoc.html.

[12] N. Tamai, "Rechargeable battery charging method," U.S. Patent US54422741995.